

58-13

SECURITY INFORMATION

CONFIDENTIAL

Copy

241

RM E53A19

53-31-6



0143422



RESEARCH MEMORANDUM

COMPARISON OF THEORETICALLY AND EXPERIMENTALLY
DETERMINED EFFECTS OF OXIDE COATINGS SUPPLIED
BY FUEL ADDITIVES ON UNCOOLED TURBINE-BLADE
TEMPERATURE DURING TRANSIENT
TURBOJET-ENGINE OPERATION

By Louis J. Schafer, Jr., Francis S. Stepka
and W. Byron Brown

Lewis Flight Propulsion Laboratory
Cleveland, Ohio

CLASSIFIED DOCUMENT

This material contains information affecting the national defense of the United States within the meaning of the Espionage Laws, Title 18, U.S.C., Secs. 793 and 794, the transmission or revelation of which in any manner to an unauthorized person is prohibited by law.

NATIONAL ADVISORY COMMITTEE FOR AERONAUTICS

WASHINGTON
March 30, 1953

**RECEIPT SIGNATURE
REQUIRED**

CONFIDENTIAL

319.98/13

ADC 901

NACA RM E53A19

1089



0143422

1Y

NACA RM E53A19

~~CONFIDENTIAL~~

NATIONAL ADVISORY COMMITTEE FOR AERONAUTICS

RESEARCH MEMORANDUMCOMPARISON OF THEORETICALLY AND EXPERIMENTALLY DETERMINED EFFECTS OF
OXIDE COATINGS SUPPLIED BY FUEL ADDITIVES ON UNCOOLED TURBINE-
BLADE TEMPERATURE DURING TRANSIENT TURBOJET-ENGINE OPERATIONBy Louis J. Schafer, Jr., Francis S. Stepka, and
W. Byron Brown

SUMMARY

An analysis was made which permitted calculation of the effectiveness of oxide coatings in retarding the transient flow of heat into turbine rotor blades when the combustion-gas temperature of a turbojet engine is suddenly changed. In order to use the analysis, it was necessary to know the coating thickness, the coating thermal conductivity, and the turbine flow conditions. An experimental investigation was made to determine the thickness of coating that will build up on the turbine blades and to check the reliability of the analysis for calculating the turbine-blade temperature response when the engine operating conditions are suddenly changed. Two fuel additives, SF-99 silicone oil and tributyl borate, were mixed with the MIL-F-5624A (grade JP-4) fuel to form coatings of silicon dioxide and boric oxide, respectively, on the turbine blades. The experimental investigation consisted in recording the transient temperature at several locations on the turbine blade while the engine was both accelerated and decelerated between the speeds of 8000 and 11,500 rpm. The engine was operated with straight JP-4 fuel as well as JP-4 fuel mixed separately with each of the fuel additives. The uncoated-blade temperature response was compared with coated-blade temperature responses to determine the effectiveness of the two coatings.

The very thin silicon dioxide and boric oxide coatings that formed on the turbine rotor blades (approximately 0.001 in.) resulted in a negligible effect on the blade temperature response. Calculations using the analysis of this report showed that for this coating thickness a coating conductivity of 0.008 Btu per hour per foot per $^{\circ}\text{F}$ would be needed to produce a lag of only 100°F in blade temperature relative to the uncoated blade 60 seconds after the engine operating conditions were changed from 8000 to 11,500 rpm. No oxide coatings are currently available with thermal conductivities this low. A comparison of experimental with calculated transient uncoated-turbine-blade temperature showed that the blade-metal temperature calculated from the analysis of this report was a maximum of 40°F lower than the experimental turbine rotor-blade

~~CONFIDENTIAL~~

ADC 901

2785

temperature during an engine acceleration from 8000 to 11,500 rpm. The use of fuel additives had no measurable effect on the engine thrust.

INTRODUCTION

The combustion-gas temperature of a turbojet engine is limited to a value which will result in a reasonable turbine-blade life. If it were possible to increase the combustion-gas temperature for a short period of time (60 sec) without the turbine-blade temperatures exceeding a limiting value, the thrust of a turbojet engine could be increased for short periods of time, provided the compressor does not surge as the engine speed and temperature are increased. A low thermal conductivity coating on the outside of the turbine blades would retard the flow of heat into the blades and thereby lengthen the time during which the extra thrust is available. Reference 1 shows that the steady-state heat-flow rate into water-cooled rocket motor walls was decreased from 30 to 50 percent by 1/8-inch-thick coatings that were applied dynamically by condensing the coating material from the products of combustion on the rocket motor walls. The analytical study reported in reference 2 shows that a 0.015-inch coating having a thermal conductivity of 0.25 Btu per hour per foot per °F would be effective in appreciably reducing the trailing-edge temperature of water-cooled turbine blades. Strong cooling existed in both references 1 and 2.

The results of an experimental investigation made to determine the effect of dynamically applied coatings of silicon dioxide and boric oxide on the transient temperature of a single, stationary, uncooled turbine blade made of S-816 alloy are reported in reference 3. In this reference transient blade temperature data were obtained on both the coated and the uncoated blade when the gas temperature was suddenly increased. The results showed a negligible effect of the coating on the rate of blade temperature response.

Although the coatings used in reference 3 were ineffective in decreasing the temperature-response rate of a stationary turbine blade, it is still desirable to be able to calculate the coating properties required for effectively retarding the transient flow of heat into gas-turbine blades when engine operating conditions are changed. Before these coating properties can be calculated, it is necessary to determine both the accuracy of the calculation method and the coating thicknesses that can be expected to form on the turbine blades. In order to determine these factors, both analytical and experimental investigations were made at the NACA Lewis laboratory.

The objectives of the analytical investigation were to obtain (1) a method of evaluating experimental data to determine the effectiveness of different coating materials in decreasing the temperature-response rate

of turbine blades and (2) an analytical method for determining the time-temperature response of a coated turbine blade. The objectives of the experimental investigation were to determine (1) the coating thickness that will occur on the turbine blades in a full-scale turbojet engine when the coating material is either silicon dioxide or boric oxide, (2) the effect of these coatings on the transient turbine-blade temperatures, (3) the accuracy with which the transient turbine-blade temperatures can be calculated from the analysis presented in this report, and (4) the effect of the coating on the engine parts and on the over-all engine performance.

The experimental investigation was made on a production turbojet engine the turbine blades of which were instrumented with thermocouples in the leading-edge, midchord, and trailing-edge regions. Transient blade temperature data for both engine acceleration and deceleration were obtained for the engine speed range from 8000 to 11,500 rpm. These speeds were chosen because they represented the extremes of combustion-gas temperature that could be obtained in the operation of the engine used in this investigation.

Two fuel additives, SF-99 silicone oil and tributyl borate, were used in the investigation to form coatings of silicon dioxide and boric oxide, respectively. Transient turbine-blade temperature data were obtained first with straight MIL-F-5624A (grade JP-4) fuel to obtain uncoated-turbine-blade data, and then similar data were obtained when each of the fuel additives was mixed with the fuel. This time-temperature data permitted the calculation of time constants (the time required for the blade temperature to increase or to decrease approximately 63 percent of the over-all difference between the initial and final blade temperatures), which were used to evaluate the effectiveness of the coatings on the blade temperature response. Data were taken during both engine acceleration and deceleration to provide additional transient temperature data for comparison with the analysis of this report.

After each fuel additive was used, the engine parts which were exposed to the combustion gases were inspected to determine the effect each coating might have on the engine parts. The effect of each coating on the engine performance was also observed during the investigation.

ANALYSIS

The strength of most turbine-blade metals decreases very rapidly with increases in the blade-metal temperature. Therefore, blade temperature increases even of short duration can cause blade failure. For this reason, if the gas temperature is to be raised above the design value, it would be convenient to be able to predict the rate of increase

of the blade temperature under the influence of the increased gas temperature. Then the time for the blade temperature to reach a critical value could be calculated. Also, if insulating coatings are used on the blade surface to retard the flow of heat into the blade, a method should be available to predict the effectiveness of these coatings in decreasing the rate of blade-metal temperature response to changes in gas temperature. Such an analysis of transient blade-metal temperatures at the midchord of both coated and uncoated blades is made in this section. A list of the symbols used in this and other sections of the report is presented in appendix A, and a similar analysis for the transient metal temperatures at the leading or trailing edges of turbine blades is given in appendix B.

2785

Uncoated Blade

For the analysis of the transient blade-metal temperatures at the midchord location, a blade section was chosen at a sufficient distance from the blade base, so that there would be no spanwise heat flow into the section. An element of this section was chosen at the midchord location where there would be no chordwise heat flow across the element boundaries. Such an element of a blade section is shown in figure 1. The length of the element is designated a (the distance between the pressure and the suction surface at the chosen location). The width of the element is b . The opposite sides of the element are assumed parallel.

The analysis considers two cases: one in which the blade-metal thermal conductivity is infinite, and one in which the blade-metal conductivity is finite. Considering the blade thermal conductivity infinite greatly simplifies the analysis; but since the turbine-blade-metal thermal conductivity is low (about 10 to 15 Btu/(ft)(hr)(°F)), the effect of the blade thermal conductivity may be significant. For this reason, both cases are considered in this analysis, and the blade temperatures calculated by both theoretical equations are compared to determine the error introduced by considering the metal thermal conductivity infinite.

Case 1 - infinite blade-metal thermal conductivity. - For this case there will be no temperature gradients across the blade section. Consider the strip of the blade section having an area ab as shown in figure 1. Let the temperature of this section be T_m . The heat received in time dt through the two surfaces of unit span that are exposed to the gas stream is

$$dQ = (h_s + h_p)b(T_{g,e,f} - T_m) dt \quad (1)$$

This heat dQ will increase the temperature of the blade strip according to the equation

$$dQ = \rho_m b a c_m \left(\frac{dT_m}{dt} \right) dt \quad (2)$$

Equating these two values of dQ (equations (1) and (2)) and solving for dt yield

$$dt = \frac{\rho_m a c_m}{(h_s + h_p)} \frac{dT_m}{T_{g,e,f} - T_m} \quad (3)$$

The boundary conditions for equation (3) are established when $t = 0$, $T_m = T_{m,i} = T_{g,e,i}$ and when $t = \infty$, $T_m = T_{m,f} = T_{g,e,f}$.

If the term $\frac{\rho_m a c_m}{h_s + h_p}$ of equation (3) is considered constant and is called τ , equation (3) can be integrated to yield

$$\frac{T_{g,e,f} - T_m}{T_{g,e,f} - T_{m,i}} = e^{-t/\tau} \quad (4)$$

The symbol τ has the dimensions of time and is usually known as the time constant. The time constant is an indication of the rate at which the blade temperature will respond to changes in the combustion-gas temperature. If the time t in equation (4) is equal to the time constant τ , the ratio $(T_{g,e,f} - T_m)/(T_{g,e,f} - T_{m,i})$ will equal approximately 0.37. This means that the time constant represents the time required for the blade temperature to increase or to decrease 63 percent of the over-all difference between the initial and final blade temperatures. Equation (4) permits the calculation of the blade-metal temperature T_m at any time t when the initial and final effective gas temperature, the blade-metal density and specific heat, the local gas-to-blade heat-transfer coefficients, and the blade geometry are known.

Case 2 - finite blade-metal thermal conductivity. - The more exact case where the blade-metal thermal conductivity is finite is now considered, so that the magnitude of the error that is introduced when blade temperatures are calculated with equation (4) can be evaluated. For the analysis, as stated previously, a strip of area of a blade section of unit depth was so chosen that no spanwise or chordwise heat flow would occur at the location. Consider such a strip of area ab of the turbine-blade section as shown in figure 1. A heat balance is made on the element of length dx of the strip of area ab . The plane 0-0 is so located that there will be no heat flow across this plane. The distance from the plane 0-0 to the suction surface is l . The distance from the plane 0-0 to the element dx is x . The rate at which

heat is transferred from the element dx through the boundary at a distance x from the plane 0-0 is

$$k_m b \frac{\partial T_m}{\partial x} \quad (5)$$

The rate at which heat is transferred through the boundary at a distance $x + dx$ is

$$k_m b \left[\frac{\partial T_m}{\partial x} + \frac{\partial}{\partial x} \left(\frac{\partial T_m}{\partial x} \right) dx \right] \quad (6)$$

The net rate at which heat is gained by the element is

$$c_m \rho_m b dx \frac{\partial T_m}{\partial t} \quad (7)$$

When this new rate of heat gain is placed equal to the difference between the rate of gain and the rate of loss from the element dx the result is

$$c_m \rho_m \frac{\partial T_m}{\partial t} = k_m \frac{\partial^2 T_m}{\partial x^2} \quad (8)$$

The thermal diffusivity of a metal is defined as $\alpha_m = \frac{k_m}{c_m \rho_m}$. Equation (8) can therefore be written as

$$\frac{\partial T_m}{\partial t} = \alpha_m \frac{\partial^2 T_m}{\partial x^2} \quad (9)$$

Since the origin plane 0-0 was chosen as a plane where $\frac{\partial T_m}{\partial x} = 0$, the plane 0-0 would fall at the center of the strip only if the heat-transfer coefficients on opposite surfaces of the blade were equal. For a turbine blade these heat-transfer coefficients are not equal, and the plane 0-0 is located near the blade surface with the lower heat-transfer coefficient. For this reason, two solutions of equation (9) are needed, one for the region between 0-0 and the suction surface of the turbine blade and the other between the plane 0-0 and the pressure surface.

Consider first the region between 0-0 and the suction surface. In order to obtain a solution of equation (9), it is convenient to introduce a new variable $\theta = T_{g,e,f} - T_m$. In terms of this variable θ , equation (9) becomes

$$\frac{\partial \theta}{\partial t} = \alpha_m \frac{\partial^2 \theta}{\partial x^2} \quad (10)$$

The boundary conditions for equation (10) are

$$(1) \text{ when } x = 0, \partial \theta / \partial x = 0$$

$$(2) \text{ when } x = l, -h_s \theta_s = k_m \left(\frac{\partial \theta}{\partial x} \right)_s$$

$$(3) \text{ when } t \rightarrow \infty, \theta \rightarrow 0$$

Assume that θ can be expressed as the product of two variables X and Y and that X is a function of x alone and Y is a function of t alone. The substitution of these values in equation (10) and the solution of the equation as presented in appendix C yield

$$\theta = \sum_{\lambda=1}^{\lambda=\infty} C e^{-\lambda^2 K^2 \alpha_m t} \cos \lambda K x \quad (11)$$

From this equation, it can be seen that the value of the time constant τ for the case of finite metal conductivity is defined by $1/\lambda^2 K^2 \alpha_m$. The integration constants C and K of equation (11) must be chosen to satisfy the three boundary conditions and also to make the two strip sections from the plane 0-0 to each surface of the blade compatible. To check boundary condition (1) differentiate equation (11) so that

$$\frac{\partial \theta}{\partial x} = \sum_{\lambda=1}^{\lambda=\infty} -K \lambda C e^{-\lambda^2 K^2 \alpha_m t} \sin \lambda K x \quad (12)$$

Thus, boundary condition (1) is satisfied for all values of C and K . Boundary condition (3) is also satisfied for all values of C and K , inasmuch as the exponential factor $e^{-\lambda^2 K^2 \alpha_m t}$ approaches zero as t becomes infinite. Substitution of equation (11) in boundary condition (2) yields

$$-h_s \sum_{\lambda=1}^{\lambda=\infty} e^{-\lambda^2 K_s^2 \alpha_m t} C_s \cos \lambda K_s l = -k_m \sum_{\lambda=1}^{\lambda=\infty} e^{-\lambda^2 K_s^2 \alpha_m t} \lambda C_s K_s \sin \lambda K_s l \quad (13)$$

Equating corresponding terms in equation (13) results in

$$\frac{h_s l}{k_m} = \lambda K_s l \tan \lambda K_s l \quad (14)$$

A transcendental equation of the same type as equation (14) is discussed in reference 4, where it is shown that there are an infinite number of roots. Reference 5 contains a table of the first six roots of this equation. For the case of the turbine blade being considered here, only the first root will be considered. Calculations using additional roots showed a negligible effect on the solution. Thus K_s is determined by the ratio $h_s l / k_m$. For the section of the strip between the plane 0-0 and the suction surface, θ_s will be given by the relation

$$\theta_s = C_s e^{-K_s^2 \alpha_m t} \cos K_s x \quad (15)$$

where K_s is defined by equation (14). The section of the strip between the plane 0-0 and the pressure surface can be treated in a similar manner. θ_p will be given by

$$\theta_p = C_p e^{-K_p^2 \alpha_m t} \cos K_p x \quad (16)$$

and K_p is defined by the relation

$$\frac{h_p(a-l)}{k_m} = K_p(a-l) \tan K_p(a-l) \quad (17)$$

If these equations are valid, they should give the same value for θ at the plane 0-0 at all times. That is,

$$C_s e^{-K_s^2 \alpha_m t} = C_p e^{-K_p^2 \alpha_m t} \quad (18)$$

To ensure this equality at all times, C_s must equal C_p and K_s must equal K_p . The value of C is determined from equation (11) when t and x equal zero. The value of K is determined by solving equations (14) and (17) simultaneously for K and l .

Coated Blade

When a low thermal conductivity coating is applied to the turbine blade, its effect appears in equation (4) or (11) as a change in the blade-surface heat-transfer coefficient. In equation (4) the heat-transfer coefficient appears in the value of τ . In equation (11) it appears in the value of K . The expression for the heat-transfer coefficient that should be used when an oxide coating is applied is presented in reference 6. This equation, in the notation of this report, is

$$\frac{1}{h_c} = \frac{1}{h} + \frac{\delta_c}{k_c} \quad (19)$$

It can be shown from the definition of the time constant and equation (19) that the change in the time constant when a coating is applied is proportional to both δ_c/k_c and h . Since the change in time constant is proportional to h , the use of low thermal conductivity coatings has a greater effect in applications where high heat-transfer coefficients exist, such as in rocket motors (ref. 1).

APPARATUS AND INSTRUMENTATION

Test Engine

The experimental portion of the investigation was conducted on a production turbojet engine which had a centrifugal compressor and a single-stage turbine. The turbine rotor blades were standard service blades made of S-816 alloy.

Fuel and Fuel Additives

The fuel used for this investigation was MIL-F-5624A (grade JP-4). Two mixtures of fuel and fuel additives were used; one contained 6 percent tributyl borate by weight and the other contained 1.2 percent silicone oil, SF-99, by weight. These mixtures produced a 1-percent concentration of boric oxide or silicon dioxide, respectively, in the products of combustion. These additives were chosen for the investigation because of their availability in the quantities desired.

Instrumentation

The engine thrust was measured with a calibrated air-cell thrust-meter. The engine speed was measured with a chronometric tachometer. The turbine rotor and stator blades were instrumented with 30-gage chromel-alumel thermocouple wire at the locations shown in figure 2. The blade thermocouples were made by threading the thermocouple leads through two-hole ceramic tubing. The ceramic tubing was inserted in a 1/16-inch-outside-diameter Inconel tube. The end of the Inconel tube was spun over to seal the thermocouple into the tube. These thermocouples were installed in radial grooves cut into the blade surface. When the thermocouples were located in the blade, the grooves were filled with a nickel-chromium brazing alloy which was then smoothed off and faired with the blade surface.

The thermocouples shown in figure 2(a) were located in three different blades so that no single blade would be excessively weakened by the grooves that were necessary for the thermocouple installation. Thermocouples 1 and 2 were located in one blade, 3 and 4 were located

in a second blade, and the thermocouples giving the spanwise temperature distribution at the blade leading edge were located in a third blade. The leads from these thermocouples were fastened to the rear face of the rotor and then led through the drilled turbine and compressor shaft to the front of the engine where they were connected to a slip-ring thermocouple pickup. A similar type thermocouple system is described in greater detail in reference 7. Two of the stator blades were instrumented as shown in figure 2(b) to obtain steady-state measurements of the spanwise temperature distributions at the leading edge of the blades and to obtain stator-blade transient temperature data. The stator-blade temperature distributions, which were obtained only during steady-state conditions, are an indication of the radial combustion-gas temperature distributions leaving the two burner liners upstream of the two instrumented stator blades. The steady-state temperature data were obtained with an indicating potentiometer, and the transient blade temperature data were obtained with recording potentiometers that drew graphs of temperature against time. Samples of these graphs are shown in figure 3.

EXPERIMENTAL PROCEDURE

The transient blade temperature data used in this report were obtained at static sea-level test conditions. The data were obtained by accelerating the engine from 8000 to 11,500 rpm (rated engine speed) and recording the turbine rotor-blade temperatures during the transition between these two operating conditions and until the blade temperatures reached equilibrium at the new conditions. The accelerations were made from the initial engine speed of 8000 rpm to the final engine speed of 11,500 rpm, because, for the turbojet engine used, acceleration through this speed range resulted in the largest difference in values of initial and final combustion-gas temperatures without exceeding rated engine speed. The engine was not accelerated above rated engine speed, because it was believed that coating thicknesses would not be sufficient to provide a blade temperature lag great enough to avoid blade failure at engine speeds above the rated value. Deceleration as well as acceleration data were recorded in this investigation, so that a comparison between the theory presented in this report and the experimental results could be made for two different types of transient heat flow. Several engine accelerations and decelerations were made with each fuel additive mixture and also with the JP-4 fuel to obtain check data and also because there were not enough recording potentiometers available to record all blade thermocouple temperatures at once. It was therefore necessary to repeat test runs with different combinations of thermocouples connected to the potentiometers.

The engine was operated first with no additive in the fuel, and data were obtained for eleven engine accelerations and seven decelerations to

2785 obtain a reference for comparisons with the coated-blade data. During these runs time-temperature relations were obtained for thermocouple locations 1, 2, 3, and 4 on the rotor blade and for location 9 on the stator blade. Silicone oil was then added to the fuel, and the engine was operated at rated engine speed for approximately 1/2 hour to provide for the coating build-up before data were taken. Eight accelerations and eight decelerations were made to obtain transient blade temperature data for the same thermocouple locations that were considered during the uncoated-blade operation. After this period of running, the engine was disassembled and the engine parts were inspected for evidences of deposits of silicon dioxide. Measurements of the coating thickness were made where thickness and uniformity of the coating permitted. The coating was then cleaned from the engine parts and the engine was reassembled. Six accelerations and six decelerations were made with the cleaned engine with JP-4 fuel used to check the first transient uncoated-blade temperature data that were obtained. The tributyl borate was then added to the fuel and the engine was operated for approximately 1/2 hour at rated speed to provide for the coating build-up. Eight accelerations and eight decelerations were then made to determine the effect of this coating on the blade temperature-time relation. Following this running, the engine parts were again inspected to determine the thicknesses and the locations of the coatings.

Each time the engine was started and before time-temperature data were obtained, the engine was operated at an engine speed of 11,500 rpm and the turbine-blade temperature was set at 1365° F by adjusting the tail-pipe nozzle opening. This procedure produced transient blade temperature data that were always between the same temperature limits and also gave about the same engine combustion-gas weight flow and thus about the same blade-surface heat-transfer coefficients. Before additives were mixed with the fuel, the engine thrust was measured to obtain a base value. During the fuel-additive investigations the engine thrust was measured to detect any change in the engine performance caused by the coatings on the turbine blades and other engine parts.

CALCULATION PROCEDURE

Theoretical Determination of Blade Time Constants

The magnitude of the time constant, as indicated in the analysis, determines the rapidity with which the blade-metal temperature responds to changes in combustion-gas temperature. Therefore, to determine the effectiveness of a coating, the terms which influence the magnitude of τ must be evaluated. For an uncoated blade, these terms are the gas-to-blade heat-transfer coefficients, blade geometry, and blade-metal conductivity, density, and specific heat. In addition, two other terms, coating conductivity and coating thickness, must be considered when the

blade is coated. In order to evaluate these terms, combustion-gas-flow conditions of a typical turbojet engine (ref. 8) were assumed. Also, in order to simplify the calculations, only a section at the blade midchord was considered.

The procedure followed in determining the terms of the time constant was as follows: The velocity distributions along the surface of the blade profile at the midspan were obtained by the use of the stream-filament theory described in reference 9. The local velocities at the midchord surfaces of the blade with the combustion-gas properties evaluated at final blade-metal temperatures were then used to determine the local convective heat-transfer coefficients on the suction and pressure surfaces by methods presented in reference 10. The values of heat-transfer coefficients thus calculated are for uncoated blades.

The effects of the coating were included by evaluating the over-all heat-transfer coefficients with equation (19) of this report. Since the coatings applied to the blade would probably be thin relative to the blade thickness (ref. 3), the effect of the coating on the velocity distribution around the blade periphery will in most cases be negligible, and it is so considered in the calculations of the convective heat-transfer coefficients in this report. However, for cases where the coating is thick, the blade profile may be altered enough to change the velocity distribution around the blade, with the result that the convective heat-transfer coefficient h would be different from that obtained for the uncoated blade. It would therefore be necessary to determine the velocity distribution and the heat-transfer coefficients for the modified profile before equation (19) could be used to determine the value of the over-all heat-transfer coefficient h_c .

The magnitudes of τ were calculated for both engine accelerations and engine decelerations by evaluating the metal density and specific heat at the final metal temperature. The blade-metal thermal conductivity was either considered infinite or evaluated at the final metal temperature.

Theoretical Determination of Effectiveness of Coatings

The theoretical effectiveness of coatings was determined by calculating, from equation (4), the blade-metal temperature variation with time for various combinations of coating thickness and coating conductivity necessary to produce a desired lag in blade-metal temperature. The value of the time constants used in equation (4) was calculated by assuming the blade-metal conductivity infinite and the same coating thickness on each surface of the blade, by neglecting the effect of coating thickness on the convective heat-transfer coefficients, and by

using values of over-all heat-transfer coefficients determined by equation (19) for various ratios of coating thickness to coating conductivity.

Method of Determining Blade Time Constants from Experimental Data

Determining the effectiveness of the coatings obtained in the experimental investigation required accurate values of the time constant because of the relatively thin coatings deposited on the blade. The calculation procedure, therefore, is so arranged as to deduce the best possible value of τ from the time-temperature data. Typical traces of the time-temperature variation at the midchord of a rotor blade as obtained with recording potentiometers are shown in figure 3.

By assuming the simple case of infinite blade-metal thermal conductivity (which, as will be shown later, varies only slightly from the more complex case of finite blade-metal conductivity) and the engine conditions as changed instantaneously, the theoretical equation of a blade temperature response with time was given in the analysis section as

$$\frac{T_{g,e,f} - T_m}{T_{g,e,f} - T_{m,i}} = e^{-t/\tau} \quad (4)$$

When the case of an uncoated blade is considered in which the blade-metal conductivity is infinite, the value of τ is given for the midchord region of the blade as

$$\tau = \frac{\rho_m a c_m}{h_s + h_p}$$

where, with the assumption that the change from one temperature level and one set of flow conditions to another is instantaneous, values of the convective heat-transfer coefficients h_s and h_p are fixed and τ is a constant. However, in the experimental investigation, approximately 6 to 15 seconds were required to change engine conditions, with the result that the heat-transfer coefficients varied and thus the value of τ also varied during the first 6 to 15 seconds. Consequently, the value of τ is determined from the data obtained after final combustion-gas-flow conditions are established or approximately 10 seconds after the time the engine speed is changed.

If equation (4) of the analysis is written in the logarithmic form,

$$\ln(T_{g,e,f} - T_m) = \ln(T_{g,e,f} - T_{m,i}) - t/\tau \quad (20)$$

it can be seen that, since $\ln(T_{g,e,f} - T_{m,i})$ is a constant, the data can be represented on a semilog plot as a straight line, if the temperature difference $(T_{g,e,f} - T_m)$ is plotted on a logarithmic scale and the time on an equal-parts scale. Equation (20) also indicates that the negative reciprocal of the slope of the line on this plot represents the value of the time constant τ . The data obtained while the engine conditions are changing will not fall on a straight line, because of the variation of the blade-surface heat-transfer coefficient during this period; however, after the engine combustion-gas-flow conditions are established, the data should fall on a straight line, as is illustrated by a typical plot of the data shown in figure 4. The intercept of the straight line on this type plot at zero time gives a fictitious value of the temperature difference $T_{g,e,f} - T_{m,i}$ that would satisfy the theoretical conditions of instantaneous change in engine conditions.

The value of τ found by this graphical method depends to some extent on judgment in fairing a line through the data and in selecting a value of $T_{g,e,f}$. The first value of $T_{g,e,f}$ usually tried is that which appears to be the final steady reading from the time-temperature traces (fig. 3). However, for some runs, after apparently reaching a final value, the final metal temperatures indicated by the traces drifted a few degrees so that the value obtained made the data incompatible with theory. A small constant error in the value of $T_{g,e,f}$, when included in a plot such as figure 4, makes the data deviate from the straight line indicated by theory. The deviation from the straight line becomes greater when time increases and $T_{g,e,f} - T_m$ decreases. The constant error in $T_{g,e,f}$ then becomes an increasingly large percentage of the temperature difference $T_{g,e,f} - T_m$. Because of this known inaccuracy in the measurement of $T_{g,e,f}$, the observed value was adjusted by a constant for any one run (never more than the instrumentation error) to produce a straight line as predicted by theory when the data is plotted as shown in figure 4.

In order to obtain as accurate a time constant from the data as possible, a method of least squares presented in appendix D was used to refine the approximate graphical results. The graphical results, because of their dependence on the observer's judgment in selecting appropriate values of $T_{g,e,f}$ and in fairing a line through the data, for some runs indicated a difference of several seconds in the value of τ as compared with values obtained with the least-square method.

RESULTS AND DISCUSSION

Experimental Time Constants

2785 Experimental time constants were determined for each of the thermocouple locations on the rotor blade and for the leading edge of the stator blade with the method of least squares outlined in appendix D. The time constants were obtained by using the transient blade temperature data for the time after the combustion-gas flow was established at the final conditions. The time constants obtained in this investigation for both accelerations and decelerations are summarized in table I. Table I(a) contains the time constants for the engine accelerations for the coated and the uncoated blades. There is some scatter of the time constants obtained from individual runs for each thermocouple location, and for this reason these values are averaged to obtain values for comparison between the coated and the uncoated blades. An inspection of the average time constants for the rotor blades reveals that for all the thermocouple locations on the turbine rotor blades the coatings of both silicon dioxide and boric oxide formed by the fuel additives (silicone oil, SF-99, and tributyl borate, respectively) had no measureable effect on the temperature response of the turbine rotor blades. The variation between the average time constants for coated and uncoated blades is of the same magnitude as the variation obtained for individual runs made on the uncoated blades. This variation between coated and uncoated blades is therefore within the experimental accuracy of the apparatus, and the effect of the coatings on the rotor blades is negligible.

The average experimental time constant for the leading edge of the uncoated stator blade was 21 seconds. The silicon dioxide coating on the stator blades increased this value to 29 seconds. This difference in time constant would result in about a 25° F decrease in the stator-blade temperature relative to the uncoated blade 60 seconds after the engine operating conditions were changed. A more complete discussion of the relation between time constants and the resulting blade temperature is presented later in this discussion. The boric oxide coating on the stator blade resulted in a time constant of 23 seconds, which was slightly higher than the uncoated-blade time constant of 21 seconds; but the difference between this value and that of the uncoated blade is within the accuracy of the experimental data.

Table I(b) contains the values of the time constants obtained when the engine was decelerated from 11,500 to 8000 rpm. These values of time constant show the same effects of the coatings as were shown in the acceleration data. The greatest effect was at the leading edge of the stator blade when the blade was coated with silicon dioxide. The deceleration time constants were larger than those obtained for engine acceleration, because the time constant is an inverse function of the local gas-to-blade-surface heat-transfer coefficient which exists at the final condition (11,500 rpm for acceleration and 8000 rpm for deceleration).

Characteristics of Coating Deposits on Blades

Inspection of the turbine blades after using each of the fuel additives showed that both coatings were very thin. This thinness was the reason for their ineffectiveness in decreasing the blade temperature-response rate. The silicon dioxide coating had a powdery appearance and showed a tendency to flake off the blades. This coating was powdery because the engine combustion-gas temperature was less than the melting point of silicon dioxide. The boric oxide coating was very thin and had a glassy appearance. The thickest coating was that of silicon dioxide on the stator blades. This inspection verified the results presented in table I, which shows that the leading edge of the stator blades had the greatest increase in the time constant. Measurements of the coating thickness were made for the silicon dioxide coating; but, because it flaked off easily and because the flow conditions over the blade were altered as the engine was shut down, the measured thicknesses are probably not the same as those that existed when the data were taken. Also, because the coatings were quite thin and powdery, it was difficult to obtain accurate measurements of the coating thickness. The boric oxide coating was so thin that it was impossible to determine the thickness that had been deposited on the rotor or the stator blades. The measured thicknesses of the silicon dioxide coating on the turbine rotor blades after the first hour of engine operation were: for the suction-surface leading edge, 0.0005 inch; midchord, 0.001 inch; and trailing edge, 0.005 inch. The pressure surface had a uniform 0.0005-inch coating over the entire surface. The leading edge of the stator blade had a 0.015-inch coating.

Comparison of Time-Temperature Curves Calculated from

Experimental Time Constants for Coated and Uncoated Blades

The average values of the experimental time constants for the stator-blade leading-edge thermocouple for the uncoated blade and the blade coated with silicon dioxide were used with equation (4) of the analysis to calculate curves of the blade temperature variation with time. The initial and final blade temperatures assumed for the calculation were 1000° F and 1365° F, respectively. These two curves are presented in figure 5. The difference in the time constants for these two curves is 8 seconds, and it is reflected in a blade temperature lag of about 25° F at a time 60 seconds after the operating conditions of the engine were suddenly changed. Similar time-temperature curves plotted for the turbine rotor-blade locations would show no difference between the coated- and the uncoated-blade curves, because of the small variations in the rotor-blade time constants which are presented in table I.

Comparisons of Theoretical and Experimental Uncoated-Blade

Time-Temperature Variations and Time Constants

Two equations, (4) and (11), derived in the analysis of this report permit the calculation of the blade temperature at any time t after the engine operating conditions have been suddenly changed. Equation (4) is based on the assumption that the thermal conductivity of the blade metal is infinite, while equation (11) is based on an assumption of a finite blade-metal thermal conductivity. These two equations were used to calculate the variation of the blade-metal temperature at the midchord, midthickness location of the uncoated turbine rotor blade for the conditions of this experimental investigation. No data from the experimental investigation were used in the calculation. The two calculated curves of the blade time-temperature relation are presented for engine acceleration and compared with an experimental curve in figure 6. The values used in obtaining the calculated curves are presented in the following table:

Blade-metal properties			Blade-surface heat-transfer coefficients, h , Btu/(sec)(sq ft)(°F)	
Density, ρ_m , lb/cu ft	Specific heat, c_m , Btu/(lb)(°F)	Thermal conductivity, k_m , Btu/(sec)(ft)(°F)	Suction- surface midchord	Pressure- surface midchord
536	0.153	0.0044	0.062	0.015

The surface heat-transfer coefficients were calculated and the blade-metal properties were evaluated as described in the CALCULATION PROCEDURE of this report. The calculated value of the heat-transfer coefficient at the suction surface is much larger than that at the pressure surface, because, for the combustion-gas-flow conditions at an engine speed of 11,500 rpm, the flow at the suction surface was turbulent while that at the pressure surface was laminar. The calculated time constants for the cases of infinite and finite blade-metal thermal conductivity were 20 and 21 seconds, respectively. These time constants were used in equations (4) and (11) to calculate the blade time-temperature relation. The time-temperature curves which were obtained with these two values of time constant are presented in figure 6.

Considering the blade-metal thermal conductivity infinite greatly simplifies the calculation of the blade-metal temperature variation and as shown in figure 6 results in a maximum difference of 6° F between the curves calculated by the two equations (4) and (11). Similarly, calculations of the magnitude of τ made for the case of engine deceleration indicated small effect due to considering the conductivity to be either finite or infinite. The computed values of τ for cases of infinite and

finite metal conductivity were 29 and 31 seconds, respectively. The larger time constant was obtained for the case of a finite blade-metal thermal conductivity which results in a finite time for the heat to flow to the midthickness location. Since the time constants obtained for the cases of finite and infinite blade-metal thermal conductivity agree, the latter, being less complex, was used in the calculations of the transient blade-metal temperatures presented in this report. The values would not agree for a blade that was considerably thicker than the blades used in this investigation or for blades of very low thermal conductivity, such as ceramic blades.

The calculated values of time constant at the midchord location and the experimental values obtained from the data after final engine combustion-gas-flow conditions were established agree very well. The calculated values as defined in equation (4) for the case of infinite thermal conductivity were 20 seconds for acceleration and 29 seconds for deceleration. The average experimental values were 20 seconds and 30 seconds for acceleration and deceleration, respectively. Therefore, a time-temperature curve calculated with the theoretical value of the time constant would be the same as one calculated with the experimental value. However, when the calculated time-temperature curve for an engine acceleration is compared with a plot of the blade temperature data against time, exact agreement between the calculated and the data curves cannot be obtained, because the engine operating conditions cannot be changed instantaneously from 8000 to 11,500 rpm as is assumed in the derivation of equation (4). A comparison between the curve calculated with equation (4) and the data curve plotted from run 14, table I(a), is shown in figure 6. The maximum difference between the two curves is about 40° F. The time required to change the engine operating conditions from 8000 to 11,500 rpm for this run was 7 seconds. The magnitude of the disagreement between the calculated and the data curve is a function of the time required to change conditions. The shorter the time required to change the operating conditions, the better will be the agreement between the calculated and the data curves.

Determination of Desired Coating Properties

The comparison between experimental and theoretical determination of turbine rotor-blade time constants shows that equation (4) is reliable for calculating the uncoated-turbine-blade time constant. It was not possible to check the reliability of equation (19) with the data of this investigation, because the coating thicknesses obtained could not be measured accurately. However, in reference 1 data are presented for the temperature reduction of rocket motor walls when they are coated with several different refractory materials. Coating-thickness data were presented only for zirconium dioxide coating. By using equation (19) it was possible to predict the reduction of heat transfer into the rocket motor walls within an accuracy of 15 percent. Therefore, equations (4)

and (19) will be used to determine the effect of different ratios of coating thickness to coating conductivity δ_c/k_c on the turbine-blade temperature response. A series of calculated time-temperature curves for a range of δ_c/k_c (from 0 to 50 (sq ft)(sec)(°F)/Btu) is presented in figure 7. These curves have been calculated for the midchord location on the blade, with the assumption that the coating thicknesses on the suction and pressure surface are the same.

2785 If, for the purpose of illustrating the shortcomings of dynamically applied oxide coatings, an arbitrary lag of the coated-blade temperature of 100° F relative to the uncoated blade is desired 60 seconds from the time the engine operating conditions are changed from 8000 to 11,500 rpm, it can be seen from figure 7 that a value of δ_c/k_c equal to about 37 (sq ft)(sec)(°F)/Btu is required for the engine combustion-gas-flow conditions used in this investigation. The silicon dioxide coating thickness required to produce this lag in turbine rotor-blade temperature could not be calculated, because the thermal conductivity of the powdered silicon dioxide deposited on the turbine blade in this investigation was unknown. Available literature gives the thermal conductivity only of fused silicon dioxide, which is higher than the powdery form that was obtained on the turbine blades. However, by using the measured values of the coating thicknesses obtained in this investigation with silicon dioxide, approximately 0.001 inch, it is possible to calculate the coating conductivity required to produce this arbitrarily desired lag in metal temperature. A coating thermal conductivity of 0.008 Btu per hour per foot per °F would be needed for a coating 0.001 inch thick. For a coating thickness of 0.010 inch, the maximum considered permissible from aerodynamic considerations of this turbine, a coating thermal conductivity of 0.08 Btu per hour per foot per °F would be required to produce the temperature lag of 100° F. A survey of literature on possible oxide coatings indicated that there were no materials available with thermal conductivities as low as 0.008 Btu per hour per foot per °F but that materials do exist with thermal conductivities in the range of 0.08 Btu per hour per foot per °F. One such material is antimony oxide, which has a conductivity of 0.068 Btu per hour per foot per °F. This oxide is a possibility for a blade-coating material if it can be dissolved in the engine fuel and if a method can be devised to cause the coating to build up to a thickness of 0.010 inch.

Deposits Formed on Engine Parts

Only the silicon dioxide deposits in the engine are presented in photographs, because the boric oxide deposits were so thin for the concentration of the additive used as to be negligible. The photographs give a clear idea of the types of coating encountered and the problems of engine operation that may result from these coatings. The silicon

dioxide coating that formed on the turbine rotor blades is shown in figure 8. The uncoated blades are shown in figure 8(a), and the blades after one hour of engine operation in figure 8(b). After this first hour of operation, the coating covered the entire blade. The coating thicknesses were measured with the coating in this condition. After an additional $1\frac{1}{2}$ hours of operation, the turbine rotor blades were coated as shown in figure 8(c). The coating did not adhere to the blades as well as it did after the first period of operation, and, as shown in figure 8(c), most of the coating on the blades had chipped off. The chipping probably resulted from loosening of the coating when the blades cooled after the first engine inspection shut-down. When the engine was started again the loosened coating was washed off.

The turbine stator blades are shown in figure 9; part (a) before engine operation and part (b) after $2\frac{1}{2}$ hours of operation. The deposit on the stator blades was heavier than on the rotor blades, but because of its thickness the coating appeared to flake off after it reached a given thickness and then to build up again. The complete washing off of the coating appears to be a characteristic only of the rotor blades, for no such complete washing was evident on the stator blades.

Photographs of the burner domes after $2\frac{1}{2}$ hours of engine operation are shown in figure 10. The burner domes were coated with a thick, spongy coating of silicon dioxide and carbon. The thickness of the deposit was about $1/8$ inch. There was also a build-up of deposit on the fuel nozzles which in time could conceivably alter the shape of the fuel spray and decrease the efficiency of combustion. The burner liners also had a deposit about 0.010 inch thick on the inside surface that was similar to that in the burner domes.

Only deposits of silicon dioxide in the engine have been discussed, because they were much greater than the boric oxide deposits formed by the additive tributyl borate. The boric oxide deposits were so slight as to be immeasurable. A characteristic of tributyl borate is its affinity for water. When it combines with water, boric oxide precipitates from the additive solution and thereby renders the additive ineffective for forming coatings on the turbine blades. This precipitate can also cause engine operating difficulties by clogging fuel filters; and, if the precipitate forms while the fuel is in the engine, difficulties such as the plugging of fuel nozzles can occur. During the operation of the engine in this investigation the fuel nozzles became plugged with the boric oxide precipitate which formed when the fuel remaining in the fuel nozzles combined with the moisture in the air after the engine was shut down for an inspection of the turbine blades. Photographs of three typical plugged fuel nozzles are compared with clean nozzles in figure 11. Nozzles number 4 and 7 were partially

plugged, and nozzle 11 was completely plugged. The plugging was severe enough to make it impossible to start the engine. After this difficulty was encountered, engine shut-downs were preceded by purging the fuel system of the engine with straight JP-4 fuel to clean the additive from the fuel nozzles. This procedure was effective in eliminating the fuel-nozzle plugging difficulties.

Effect of Fuel Additives on Engine Performance

The use of either SF-99 silicone oil or tributyl borate as an additive in the fuel for a period of approximately 2 hours of engine operation did not cause a measurable change in the engine thrust, as compared with an engine operating on JP-4 fuel with no additive. There also was no change in the burner-outlet spanwise temperature distribution resulting from the addition of the silicone oil, SF-99, or the tributyl borate to the fuel. The only change in the engine performance was an increase in the specific liquid (fuel plus additive) consumption. This change was a result of depression of the heating value of the JP-4 fuel by the low heating values of the additives, which made a higher fuel-air ratio necessary to obtain the required turbine-inlet temperature at rated engine speed of 11,500 rpm.

SUMMARY OF RESULTS

An analysis was made to permit the prediction of the temperature response of coated and uncoated uncooled turbine rotor blades after a sudden change in the combustion-gas temperature. An experimental investigation was made on a turbojet engine to check the analysis and to determine the effectiveness of dynamically applied coatings of silicon dioxide and boric oxide. The fuel additives used to produce these coatings were silicone oil, SF-99, and tributyl borate, respectively. The mixtures of these additives with the fuel produced a 1-percent concentration of the coating material in the products of combustion. The results of this investigation are as follows:

1. Neither the silicon dioxide nor the boric oxide coating on the turbine rotor blades was effective in retarding the rate of turbine-blade temperature response.
2. The analysis permitted calculation of the experimental transient turbine-blade temperatures of this investigation with a maximum error of about 40° F.
3. For the coating thickness obtained with silicon dioxide at the midchord location (0.001 in.) the analysis indicated that a coating thermal conductivity of 0.008 Btu per hour per foot per °F would be

needed to produce a blade temperature lag of 100°F 60 seconds after the engine operating conditions were changed from 8000 to 11,500 rpm. A survey of literature showed that no oxide coatings having conductivities this low are available.

4. For the maximum coating thickness (0.010 in.) that can be permitted on the turbine blade from aerodynamic considerations, the analysis indicated that, for the metal temperature lag of 100°F 60 seconds after the engine operating conditions were changed, a coating thermal conductivity of 0.08 Btu per hour per foot per $^{\circ}\text{F}$ was needed. A survey of literature indicated that only few oxides have thermal conductivities this low. Antimony oxide is one that falls in this range and is a possibility for a blade-coating material if it can be used with the dynamic coating technique and if it will deposit on the turbine-rotor blades to a thickness of 0.010 inch.

5. Engine operation for a period of approximately 2 hours with each fuel additive and the resulting deposits on the engine parts had no measurable effect on the engine thrust.

Lewis Flight Propulsion Laboratory
National Advisory Committee for Aeronautics
Cleveland, Ohio

582

APPENDIX A

SYMBOLS

The following symbols are used in this report:

- 2785
- A area of blade leading-edge section, sq ft
- a length of element at midchord of blade, ft
- b width of element at midchord of blade, ft
- C integration constant
- c specific heat, Btu/(lb)(°F)
- h local gas-to-blade-surface heat-transfer coefficient,
Btu/(sec)(sq ft)(°F)
- \bar{h} average gas-to-blade heat-transfer coefficient over length L of
blade leading edge, Btu/(sec)(sq ft)(°F)
- K integration constant
- k thermal conductivity, Btu/(sec)(ft)(°F)
- L length of leading-edge periphery exposed to gas stream, ft
- l distance from plane O-O to suction surface, ft
- M intersection of suction surface and plane which separates leading
edge from remainder of blade
- N intersection of pressure surface and plane which separates leading
edge from remainder of blade
- n direction normal to boundary MN
- O-O plane through blade element where $dT_m/dx = 0$
- Q heat flow, Btu
- s length of leading-edge boundary, ft
- T temperature, °F
- t time, sec

- X function of x
- x distance from plane 0-0 to incremental element of blade midchord section, ft
- Y function of t
- α thermal diffusivity $k/\rho c$, sq ft/sec
- Δ correction to $T_{g,e,f,o}$
- δ thickness, ft
- ϵ correction to τ_o
- θ $(T_{g,e,f} - T_m)$, $^{\circ}F$
- λ index of summation
- ρ density, lb/cu ft
- τ time constant $\rho ac/h$, sec

Subscripts:

- c coated
- e effective
- f final
- g combustion gas
- i initial
- m metal
- o values obtained by approximate graphical method
- p pressure surface
- s suction surface
- l applied to integration constants

APPENDIX B

ANALYSIS OF TRANSIENT METAL TEMPERATURES AT LEADING OR
TRAILING EDGES OF TURBINE BLADES

2785
The equations presented in this section are derived only for the leading edge of the turbine blade, but they also may be applied to the trailing edge. The only differences between these two locations are the blade geometry and the gas-to-blade heat-transfer coefficients.

Uncoated Blade

Consider a section of the leading edge of a turbine blade as shown in figure 1. This section has unit span, area A , and length L , of the periphery exposed to the exhaust gas. The plane M-N separates the leading-edge section from the rest of the blade. It is chosen such that the chordwise heat flow from the leading edge is perpendicular to the plane at all points. The direction of heat flow is n , and an element of blade in the direction of heat flow is dn .

The net heat flow into the area A through the boundaries must equal the heat stored in the area. Such a heat balance results in the equation

$$\int_{L=0}^{L=L} h(T_{g,e,f} - T_m) dL + k_m \int_M^N \left(\frac{dT_m}{dn} \right) ds = \rho_m A c_m \left(\frac{dT_m}{dt} \right) \quad (B1)$$

from which

$$dt = \frac{\rho_m A c_m dT_m}{\int_{L=0}^{L=L} h(T_{g,e,f} - T_m) dL + k_m \int_M^N \left(\frac{dT_m}{dn} \right) ds} \quad (B2)$$

$$= \frac{\rho_m A c_m dT_m}{(T_{g,e,f} - T_m) \int_{L=0}^{L=L} h dL + k_m \int_M^N \left(\frac{dT_m}{dn} \right) ds} \quad (B3)$$

If the boundary M-N is chosen so that $(dT_m/dn)ds$ is zero or negligible, the term $k_m \int_M^N \left(\frac{dT_m}{dn} \right) ds$ can be neglected (the case of infinite blade-metal thermal conductivity). Also, if $\int_{L=0}^{L=L} h(dL)$ can be evaluated in terms of an average heat-transfer coefficient \bar{h} for the length L of the leading-edge surface exposed to the gas stream, then

$\int_{L=0}^{L=L} h(dL) = \bar{h}L$, and equation (B3) can be written

$$dt = \frac{\rho_m A c_m dT_m}{\bar{h}L(T_{g,e,f} - T_m)} \quad (B4)$$

The time constant for the leading edge of the blade then is defined as

$$\tau = \frac{\rho_m A c_m}{\bar{h}L} \quad (B5)$$

and integration of equation (B4) will again produce equation (4)

$$\frac{T_{g,e,f} - T_m}{T_{g,e,f} - T_{m,i}} = e^{-t/\tau} \quad (4)$$

If the heat flow across the boundary M-N cannot be neglected (the case of a finite blade-metal thermal conductivity), then the term

$k_m \int_M^N \left(\frac{dT_m}{dn} \right) ds$ must be included in the time constant. The time constant is then

$$\tau = \frac{\rho_m A c_m}{\bar{h}L \left[1 + \frac{k_m \int_M^N \left(\frac{dT_m}{dn} \right) ds}{\bar{h}L(T_{g,e,f} - T_m)} \right]} \quad (B6)$$

Coated Blade

The effect of an oxide coating on the leading and the trailing edge of a turbine blade is handled the same as the coating on the midchord location. Equation (19) is used to calculate the over-all heat-transfer

coefficient for the leading edge of the coated blade. This coefficient is then used in equation (B5) or (B6) to determine the time constant, which is then used with equation (4) to determine the leading-edge blade temperature at any time t after engine operating conditions have been changed.

2785

APPENDIX C

SOLUTION OF DIFFERENTIAL EQUATION FOR TRANSIENT BLADE TEMPERATURE WHEN
BLADE-METAL THERMAL CONDUCTIVITY IS FINITE

When the turbine-blade-metal thermal conductivity is considered finite in the calculations of the transient turbine-blade temperature after the turbine operating conditions have been changed, it is necessary to solve the differential equation

$$\frac{\partial \theta}{\partial t} = \alpha_m \frac{\partial^2 \theta}{\partial x^2} \quad (10)$$

The solution of this differential equation is presented here. The boundary conditions for the equation are

$$\text{when } x = 0, \partial \theta / \partial x = 0$$

$$\text{when } x = l, -h_s \theta_s = k_m \left(\frac{\partial \theta}{\partial x} \right)_s$$

$$\text{when } t \rightarrow \infty, \theta \rightarrow 0$$

Assume that θ can be expressed as the product of two variables X and Y , where X is a function of x and Y is a function of t . Thus

$$\theta = X \cdot Y \quad (C1)$$

Substitution of this value of θ in equation (10) yields

$$\frac{dY}{dt} X = \alpha_m Y \left(\frac{d^2 X}{dx^2} \right) \quad (C2)$$

or

$$\frac{1}{Y} \frac{dY}{dt} = \frac{\alpha_m}{X} \frac{d^2 X}{dx^2} \quad (C3)$$

Since the left term of equation (C3) is a function of t , and the right term is a function of x , both terms are constant and equal. This constant value can be written as $-K^2 \alpha_m$. Equation (C3) can now be written as two ordinary differential equations

$$\frac{1}{Y} \frac{dY}{dt} = -K^2 \alpha_m \quad (C4)$$

and

$$\frac{1}{X} \frac{d^2 X}{dx^2} = -K^2 \quad (C5)$$

These two equations can be rewritten as

$$\frac{dY}{Y} = -K^2 \alpha_m dt \quad (C6)$$

and

$$\frac{d^2 X}{dx^2} + K^2 X = 0 \quad (C7)$$

Equation (C6) can be integrated to produce

$$\ln Y = -K^2 \alpha_m t + \ln Y_1$$

or

$$Y = Y_1 e^{-K^2 \alpha_m t} \quad (C8)$$

Equation (C7) is a simple harmonic equation and its solution can be written in a number of forms. The one best adapted to the present boundary conditions is

$$X = X_1 \cos Kx \quad (C9)$$

A solution of equation (C1) can then be written as

$$\theta = Y_1 X_1 e^{-K^2 \alpha_m t} \cos Kx \quad (C10)$$

The product $X_1 Y_1$ is a constant of integration to be determined from the boundary conditions. It is numerically equal to the temperature difference θ at the plane 0-0 when $t = 0$ and is defined as a constant C . Because equation (C10) is only one solution of the linear equation and any combination of solutions of the equation is also a solution, equation (C10) in its most general form can be written as

$$\theta = \sum_{\lambda=1}^{\lambda=\infty} C e^{-\lambda^2 K^2 \alpha_m t} \cos \lambda Kx \quad (11)$$

APPENDIX D

METHOD OF LEAST SQUARES AS APPLIED TO APPROXIMATE GRAPHICAL RESULTS
FOR DETERMINATION OF TIME CONSTANTS

The procedure followed to obtain the time constants from the experimental data is presented herein. Equation (4) is solved for T_m and becomes

$$T_m = T_{g,e,f} - (T_{g,e,f} - T_{m,i})e^{-t/\tau} \quad (D1)$$

The quantities to be determined are $T_{g,e,f}$ and τ . These terms are to be given magnitudes which make the sums of the squares of the residuals a minimum. A residual is the temperature difference $(T_{m,o} - T_m)$, where

$$T_{m,o} = T_{g,e,f,o} - (T_{g,e,f,o} - T_{m,i})e^{-t/\tau_o} \quad (D2)$$

Because equation (D1) is not linear in T , but transcendental, it will be linearized by means of Taylor's theorem for two independent variables. Let

$$\tau = \tau_o + \epsilon$$

and

$$T_{g,e,f} = T_{g,e,f,o} + \Delta$$

where τ_o and $T_{g,e,f,o}$ are the values found by the approximate graphical method, and ϵ and Δ are the corrections to be made so as to minimize the sum of the squares of the residuals. Then by Taylor's theorem,

$$T_m = T_{m,o} + \Delta \left(\frac{\partial T_m}{\partial T_{g,e,f}} \right)_o + \epsilon \left(\frac{\partial T_m}{\partial \tau} \right)_o + \dots \quad (D3)$$

This equation is linear in Δ and ϵ if these corrections are small enough that the terms involving the higher powers of them, such as Δ^2 , $\epsilon\Delta$, ϵ^2 , and so forth, can be neglected. All the terms in equation (D3) can be obtained from the data except the two unknowns Δ and ϵ .

The values of Δ and ϵ that render the sum of the squares of the residuals a minimum are given in reference 11 as

$$\left. \begin{aligned} & \left[\sum \left(\frac{\partial T_m}{\partial T_{g,e,f}} \right)_o^2 \right] \Delta + \left[\sum \left(\frac{\partial T_m}{\partial T_{g,e,f}} \right)_o \left(\frac{\partial T_m}{\partial \tau} \right)_o \right] \epsilon + \sum (T_{m,o} - T_m) \left(\frac{\partial T_m}{\partial T_{g,e,f}} \right)_o = 0 \\ & \left[\sum \left(\frac{\partial T_m}{\partial T_{g,e,f}} \right)_o \left(\frac{\partial T_m}{\partial \tau} \right)_o \right] \Delta + \left[\sum \left(\frac{\partial T_m}{\partial \tau} \right)_o^2 \right] \epsilon + \sum (T_{m,o} - T_m) \left(\frac{\partial T_m}{\partial \tau} \right)_o = 0 \end{aligned} \right\} \quad (D4)$$

In equations (D4) the value of the blade-metal temperature T_m is obtained from the time-temperature data, while other terms are obtained by solving or differentiating equation (D2). By inserting the values of these terms obtained for each data point, the products and accumulations required in equation (D4) can be computed and the equations solved for Δ and ϵ . The values of $T_{g,e,f,o}$ and τ_o obtained by the approximate graphical method then can be corrected by Δ and ϵ , respectively, to obtain the corrected values of $T_{g,e,f}$ and τ .

REFERENCES

1. Thomas, Delbert D., and Cole, Leland G.: The Reduction of Heat Transfer to Rocket Motors by Motor-Wall-Coating Techniques. Prog. Rep. No. 9-50, Jet. Prop. Lab., C.I.T., Dec. 15, 1950. (ORDCIT Proj. Contract No. DA-04-495-ORD 18.)
2. Brown, W. Byron, and Livingood, John N. B.: Cooling of Gas Turbines. IX - Cooling Effects from Use of Ceramic Coatings on Water-Cooled Turbine Blades. NACA RM E8H03, 1948.
3. McCafferty, Richard J., and Butze, Helmut F.: Temperature Response of Turbine-Blade Metal Covered with Oxide Coatings Supplied by Fuel Additives. NACA RM E52G07, 1952.
4. Harper, D. R., 3d, and Brown, W. B.: Mathematical Equations for Heat Conduction in the Fins of Air-Cooled Engines. NACA Rep. 158, 1922.
5. Carslaw, H. S., and Jaeger, J. C.: Conduction of Heat in Solids. The Clarendon Press (Oxford), 1947, p. 377.
6. McAdams, William H.: Heat Transmission. 2d ed., McGraw-Hill Book Co., Inc., 1942, p. 136.

7. Ellerbrock, Herman H., Jr., and Stepka, Francis S.: Experimental Investigation of Air-Cooled Blades in Turbojet Engine. I - Rotor Blades with 10 Tubes in Cooling-Air Passages. NACA RM E50I04, 1950.
8. Ayer, E. L.: Basis of Correction of Test Results and Extrapolation to Altitude Conditions for Type I Jet-Propulsion Aircraft Gas Turbines. Bull. No. DF81407, Aircraft Gas Turbine Eng. Div., General Electric Co., Oct. 1, 1945.
9. Hubbartt, James E., and Schum, Eugene F.: Average Outside-Surface Heat-Transfer Coefficients and Velocity Distributions for Heated and Cooled Impulse Turbine Blades in Static Cascades. NACA RM E50L20, 1951.
10. Brown, W. Byron, and Donoughe, Patrick L.: Extension of Boundary-Layer Heat-Transfer Theory to Cooled Turbine Blades. NACA RM E50F02, 1950.
11. Merriman, Mansfield: Method of Least Squares. John Wiley & Sons, Inc., 1915.

2785

TABLE I. - TABULATION OF BLADE TIME CONSTANTS



(a) Data obtained by accelerating engine from 8000 to 11,500 rpm.

Run	Time constant, τ , sec				
	Rotor-blade thermocouple location				Stator-blade thermocouple location
	Leading edge	Trailing edge	Midchord suction surface	Midchord midthickness	Leading edge
MIL-F-5624A (grade JP-4) fuel					
1	19	24	--	22	--
2	19	22	--	19	--
3	20	24	--	20	--
4	--	24	20	19	--
5	--	--	22	23	--
6	22	--	20	21	--
7	--	--	--	17	--
8	24	--	23	21	--
9	20	--	--	21	17
10	--	--	--	22	18
11	--	--	--	--	20
12	--	--	--	24	--
13	19	22	--	22	--
14	24	25	--	19	--
15	19	--	23	20	23
16	--	--	20	18	24
17	21	--	21	19	23
Average	21	23	21	20	21
MIL-F-5624A (grade JP-4) fuel plus 1.2 percent by weight of silicone oil, SF-99					
1a	20	22	23	--	27
2a	--	22	22	--	28
3a	20	--	25	--	29
4a	20	--	21	--	27
5a	--	--	18	--	23
6a	20	--	19	--	30
7a	23	--	19	--	32
8a	--	--	--	--	37
Average	21	22	21	--	29
MIL-F-5624A (grade JP-4) fuel plus 6 percent by weight of tributyl borate					
1b	22	--	23	21	20
2b	23	--	24	23	21
3b	20	--	22	22	28
4b	--	25	25	22	22
5b	19	22	19	--	22
6b	17	19	19	--	--
7b	19	22	21	--	23
8b	--	20	--	--	--
Average	20	22	22	22	23

TABLE I. - TABULATION OF BLADE TIME CONSTANTS - Concluded

(b) Data obtained by decelerating engine from 11,500 to 8000 rpm.

Run	Time constant, τ , sec				
	Rotor-blade thermocouple location				Stator-blade thermocouple location
	Leading edge	Trailing edge	Midchord suction surface	Midchord midthickness	Leading edge
MIL-F-5624A (grade JP-4) fuel					
1	30	35	--	31	--
2	27	34	--	28	--
3	27	31	--	28	--
4	30	33	30	28	--
5	29	--	30	30	--
6	27	--	--	28	30
7	28	--	--	29	31
8	30	34	--	32	--
9	33	32	--	32	--
10	29	30	--	29	--
11	31	--	33	31	34
12	32	--	32	30	--
13	31	--	31	30	--
Average	30	33	31	30	32
MIL-F-5624A (grade JP-4) fuel plus 1.2 percent by weight of silicone oil, SF-99					
1a	31	33	33	--	--
2a	30	32	31	--	32
3a	31	--	--	--	33
4a	27	35	30	--	29
5a	31	--	31	--	36
6a	34	--	29	--	37
7a	34	36	33	--	40
8a	30	--	31	--	41
Average	31	34	31	--	35
MIL-F-5624A (grade JP-4) fuel plus 6 percent by weight of tributyl borate					
1b	34	--	32	31	33
2b	36	--	36	33	30
3b	32	--	32	31	--
4b	--	31	32	31	--
5b	29	--	--	--	31
6b	28	29	28	--	33
7b	28	28	28	--	31
8b	--	29	--	--	36
Average	31	29	31	32	32

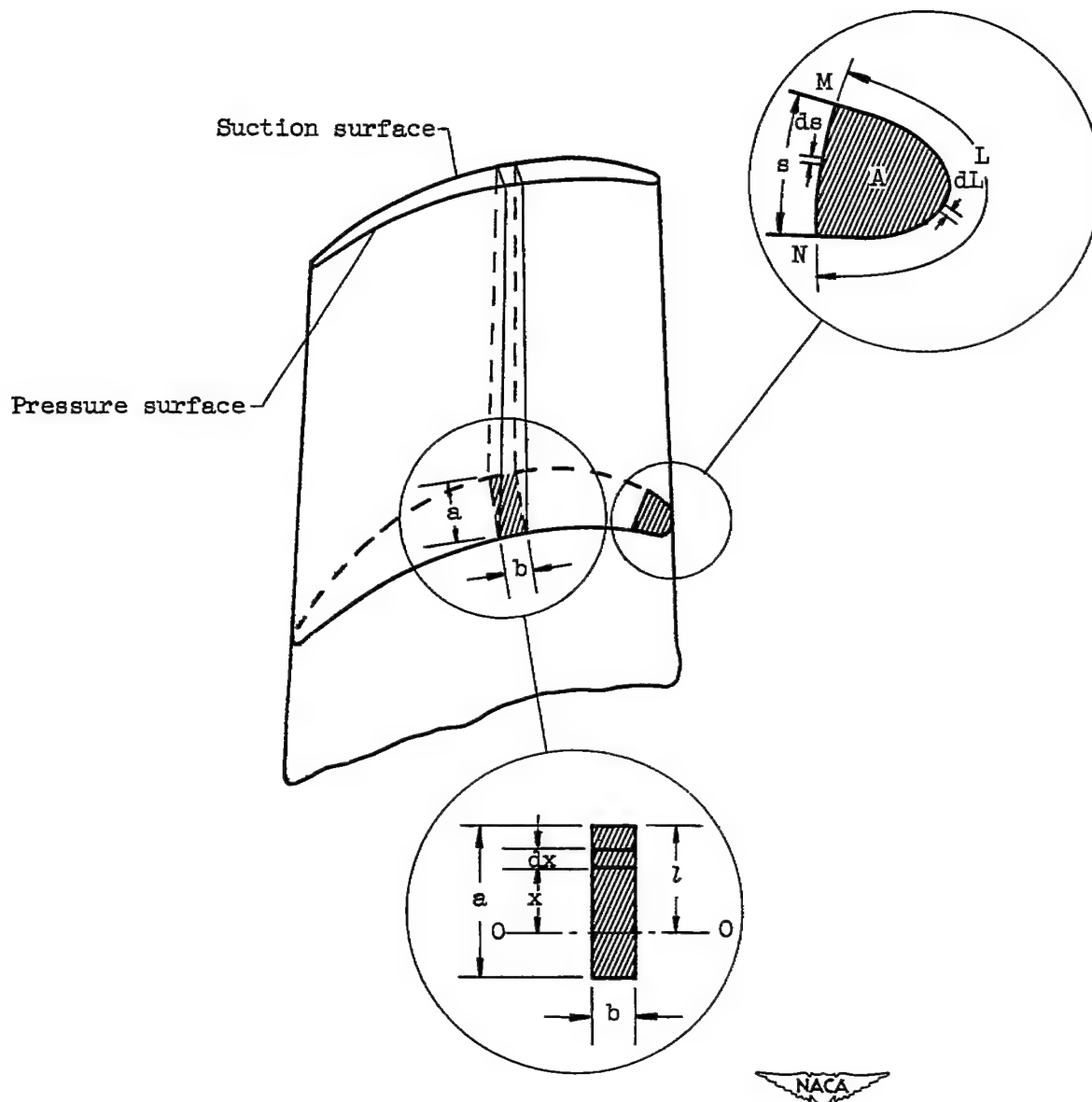
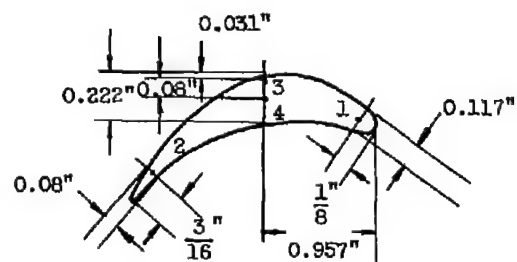
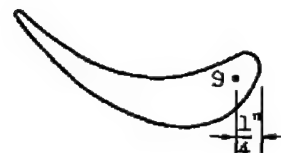


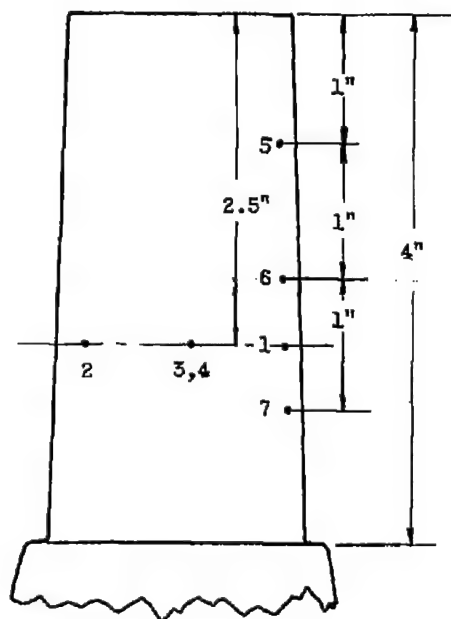
Figure 1. - Turbine-blade areas considered in analytical development of blade time constants.



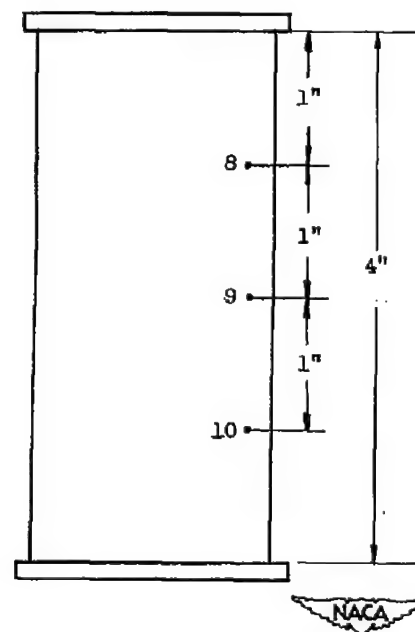
Cross section at $2\frac{1}{2}$ in. from tip



Cross section at 2 in. from tip



(a) Rotor blade.

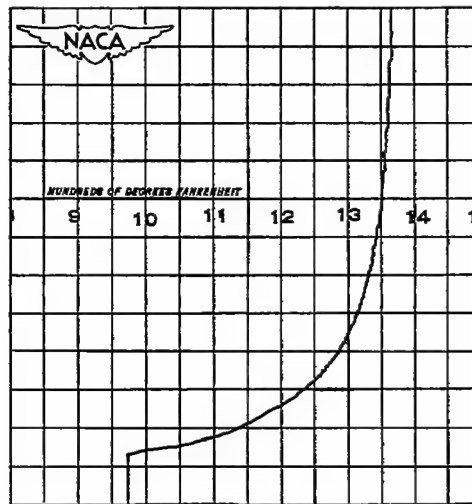


(b) Stator blade.

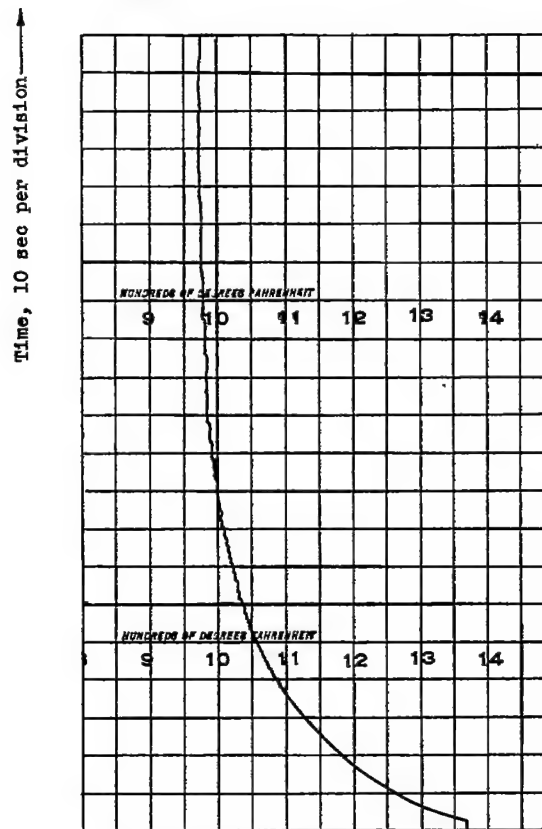
Figure 2. - Locations of thermocouples on turbine rotor and stator blades.

CONFIDENTIAL

NACA RM E53A19

~~CONFIDENTIAL~~

(a) Acceleration; run 14. Thermocouple located at midchord, midthickness of blade.



(b) Deceleration; run 9. Thermocouple located at midchord, midthickness of blade.

Figure 3. - Typical time-temperature traces of uncoated-rotor-blade temperature obtained with recording potentiometers.

~~CONFIDENTIAL~~

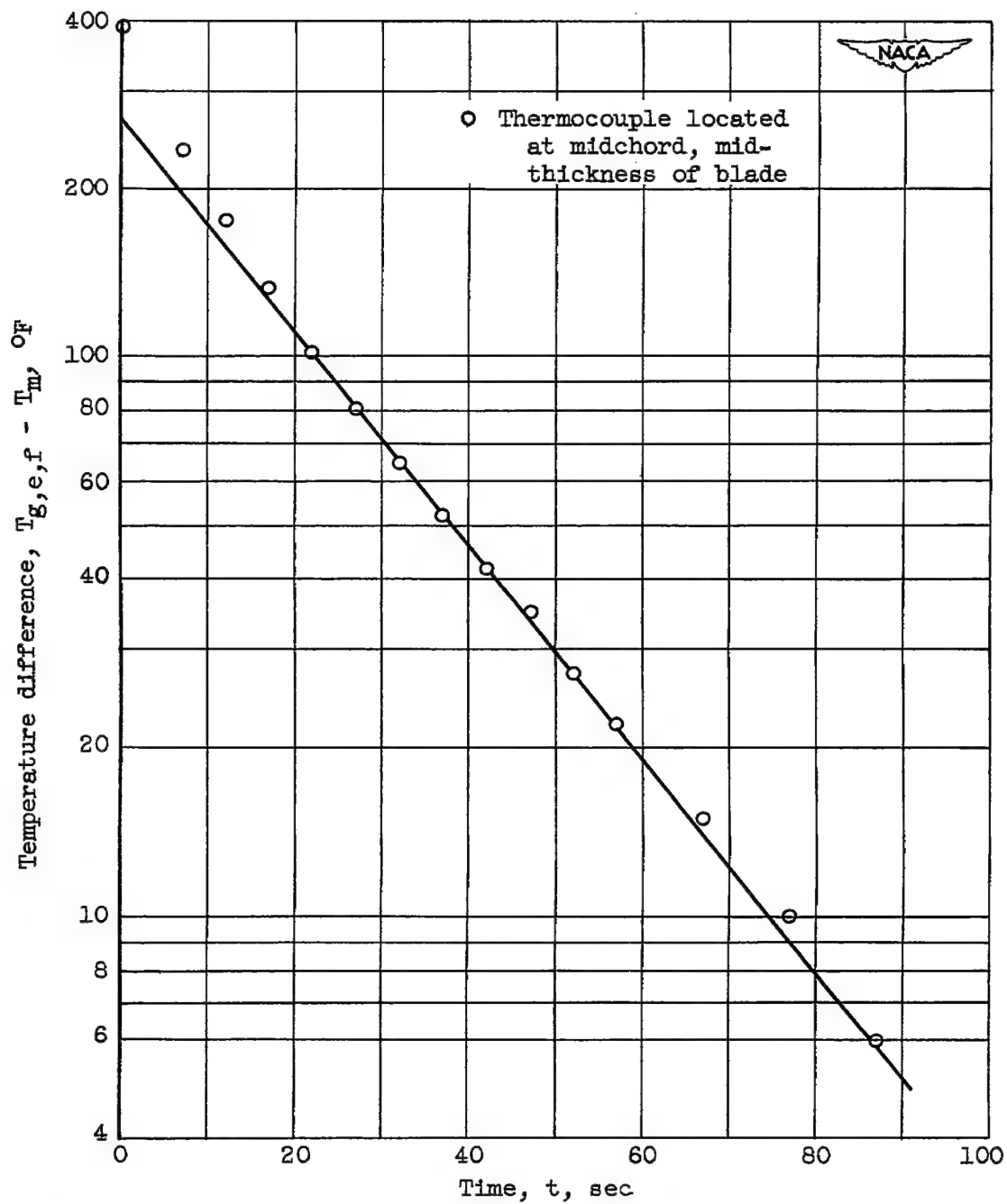
~~CONFIDENTIAL~~

Figure 4. - Typical plot of blade temperature data for determination of time constants. Acceleration; run 14.

~~CONFIDENTIAL~~

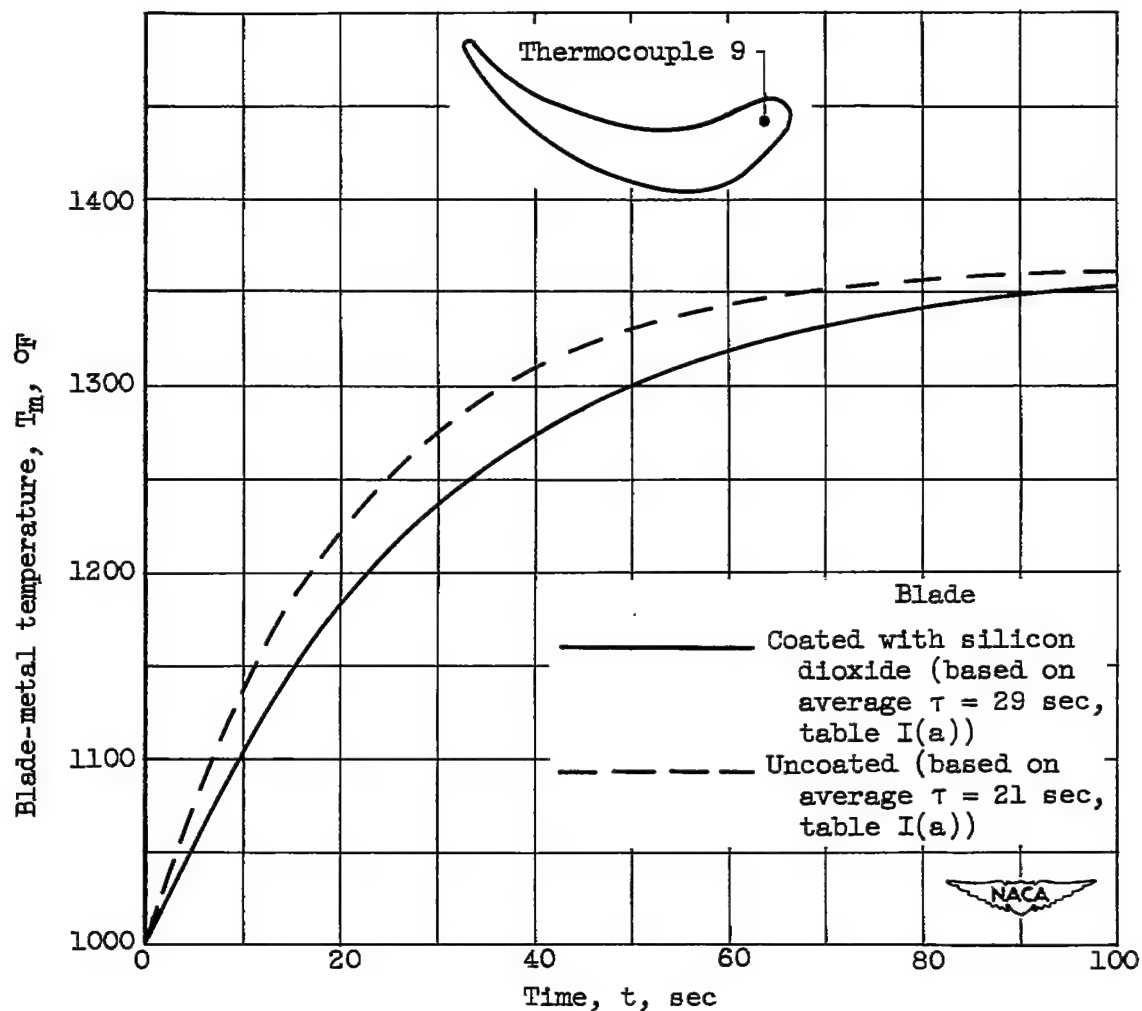


Figure 5. - Comparison of calculated stator-blade time-temperature relations for uncoated blade and blade coated with silicon dioxide. Curves calculated with experimental time constants in equation (4); blade-metal initial temperature, 1000° F; blade-metal final temperature, 1365° F.

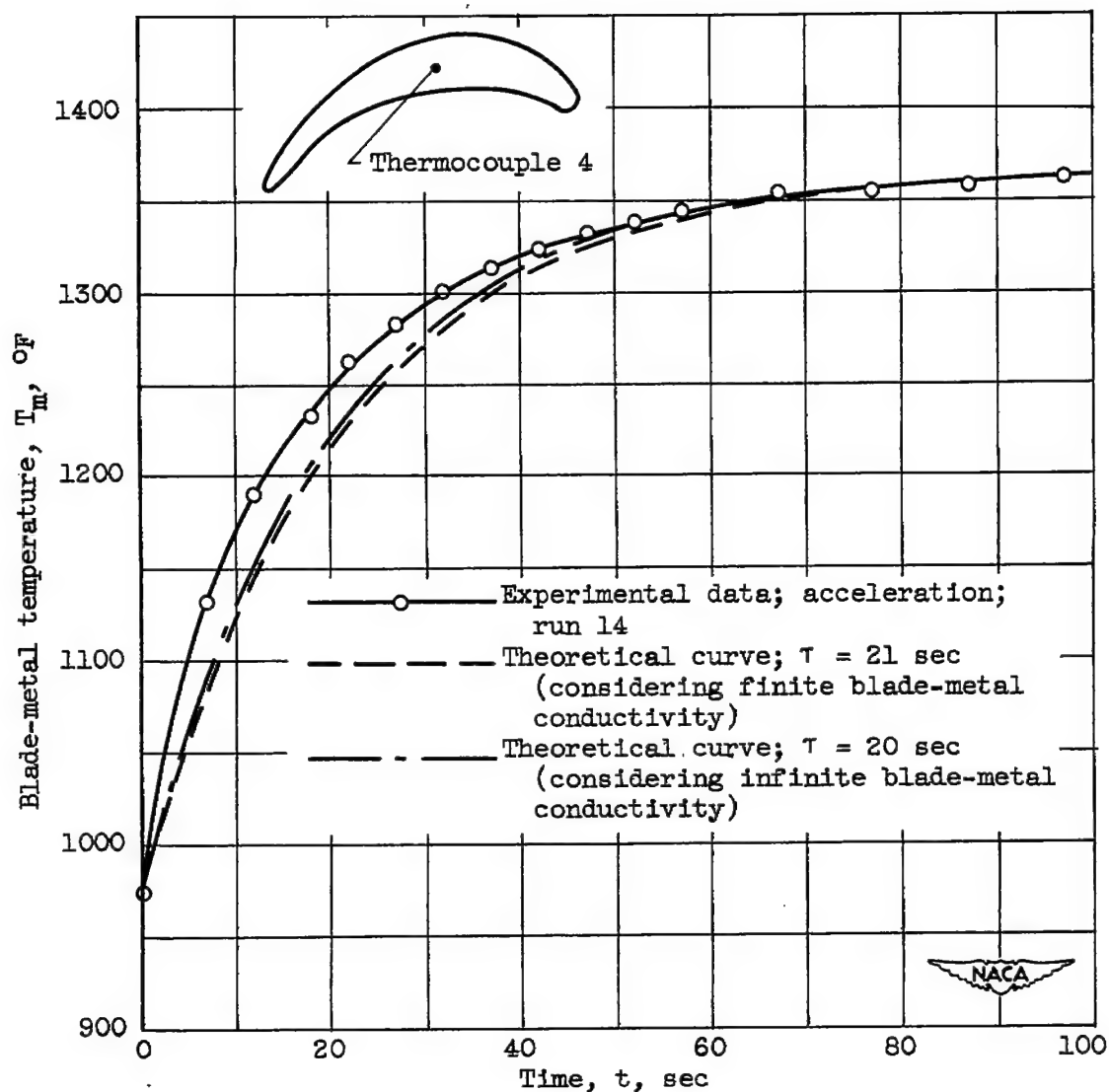


Figure 6. - Comparison of experimental and theoretical time-temperature relations at midchord, midthickness of uncoated rotor blade. Blade-metal initial temperature, 972°F ; blade-metal final temperature, 1365°F .

CONFIDENTIAL

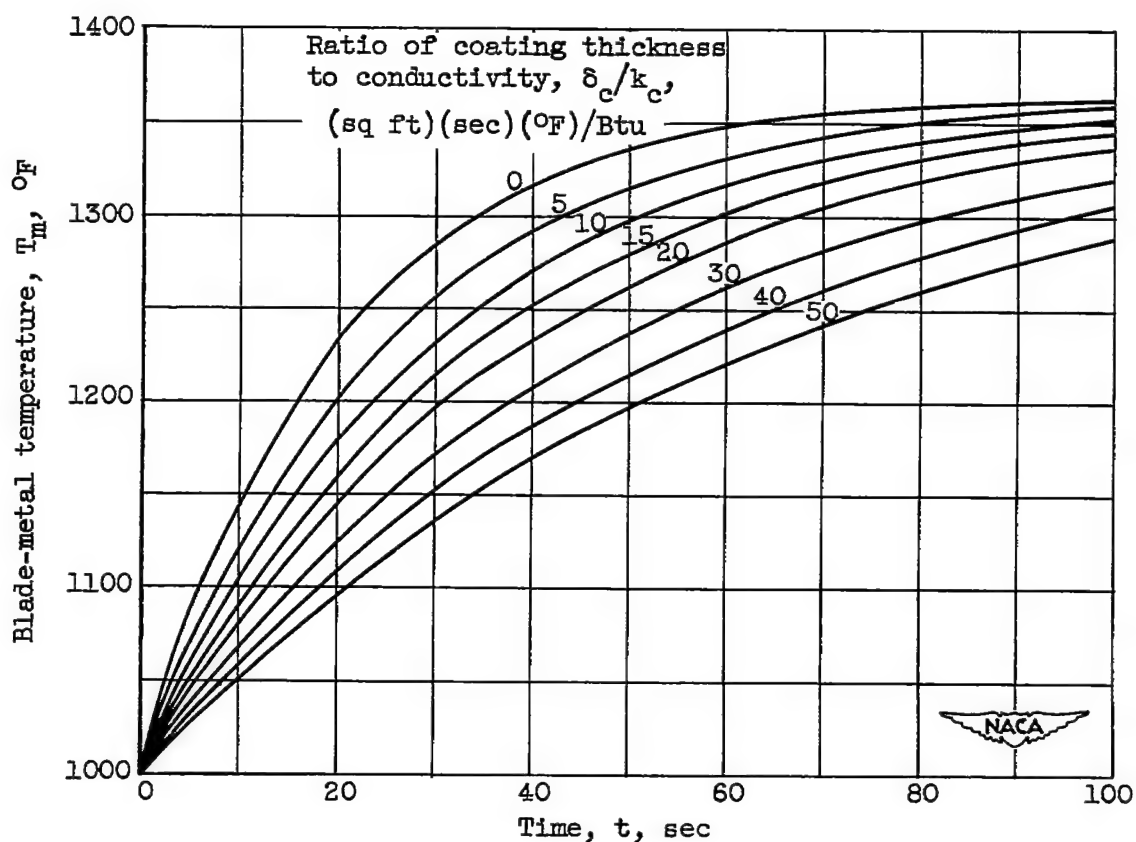
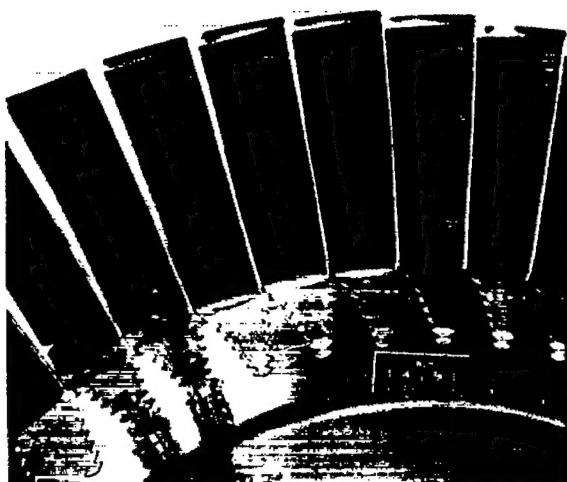
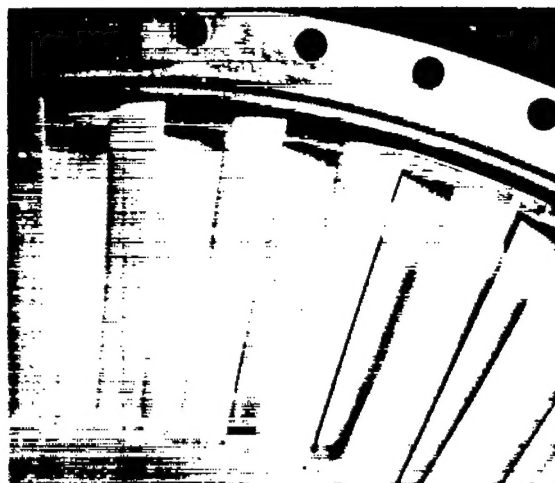


Figure 7. - Theoretical variation of time-temperature relation at blade midchord with ratios of coating thickness to coating conductivity. Blade-metal thermal conductivity considered infinite; blade-metal initial temperature, 1000° F; blade-metal final temperature, 1365° F.

CONFIDENTIAL

~~CONFIDENTIAL~~

(a) Blades before operation.



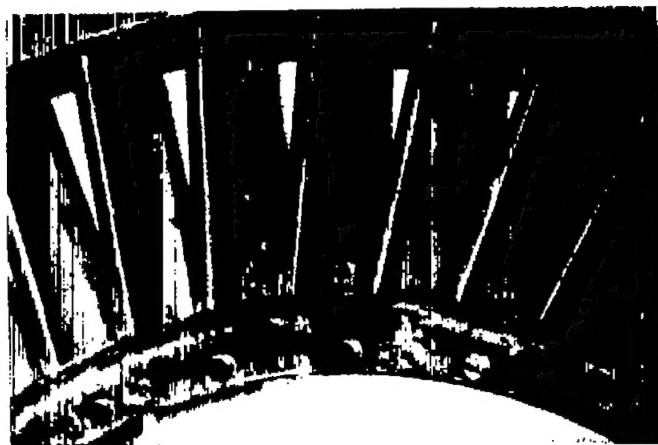
(b) Blades after 1 hour of operation.

(c) Blades after $2\frac{1}{2}$ hours of operation.

Figure 8. - Turbine rotor blades before and after operation with silicone oil, SF-99, added to the fuel.


C-31586~~CONFIDENTIAL~~

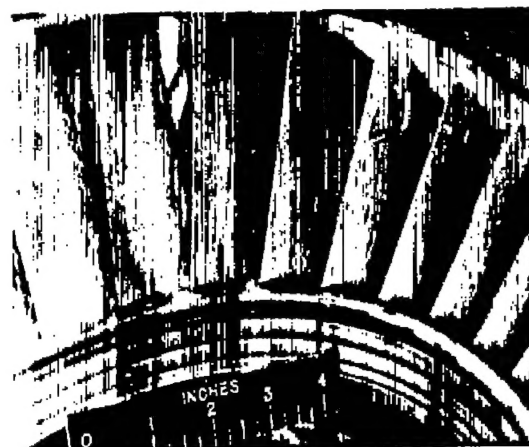
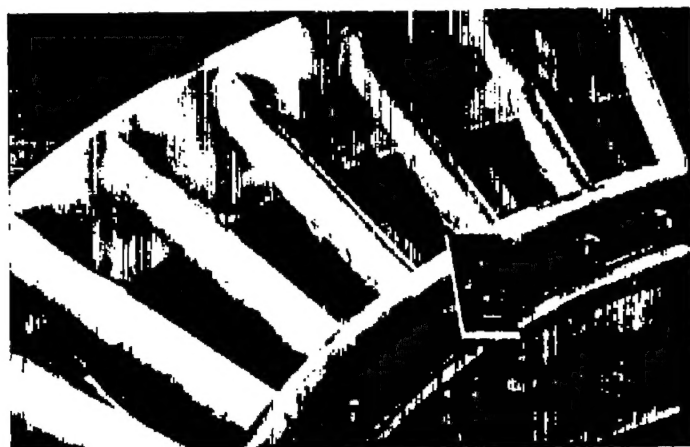
Leading edge of blades



Trailing edge of blades



(a) Blades before operation.



(b) Blades after $2\frac{1}{2}$ hours of operation.

Figure 9. - Stator blades before and after operation with silicone oil, SF-99, added to the fuel.

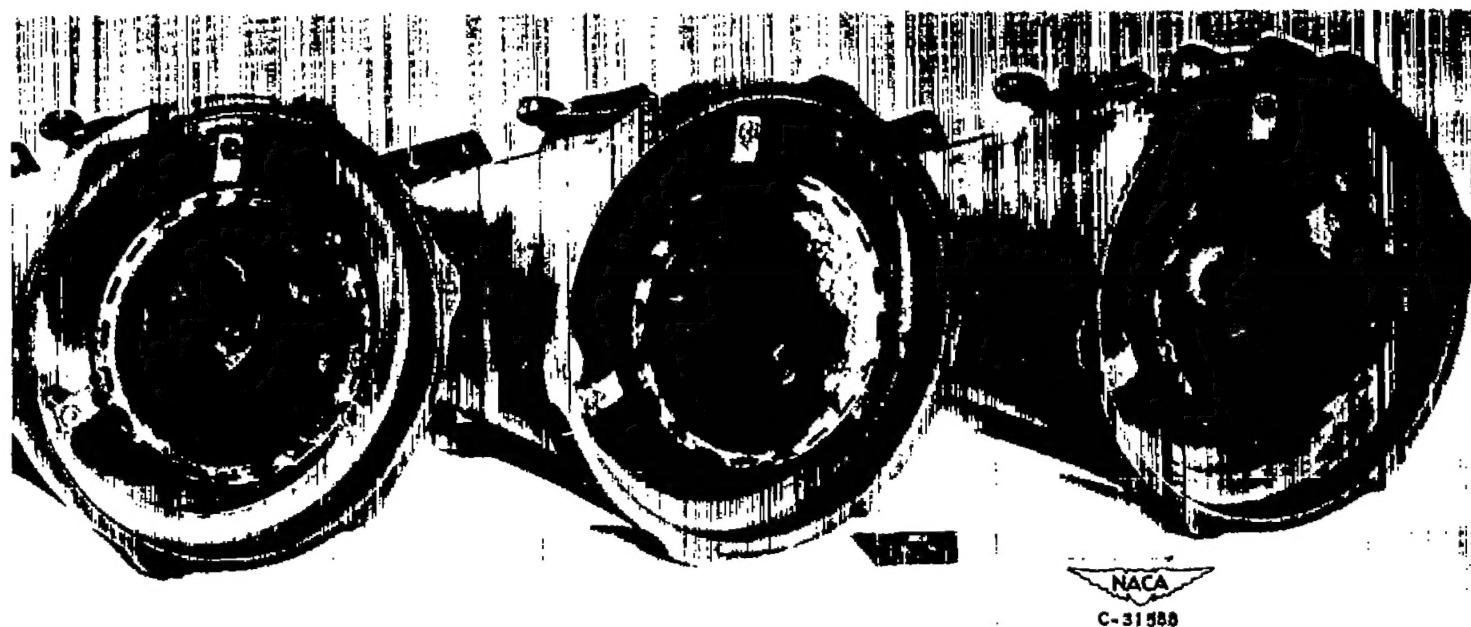


Figure 10. - Silicon dioxide and carbon deposits on burner domes after approximately $2\frac{1}{2}$ hours of operation with silicone oil, SF-99, added to the fuel.

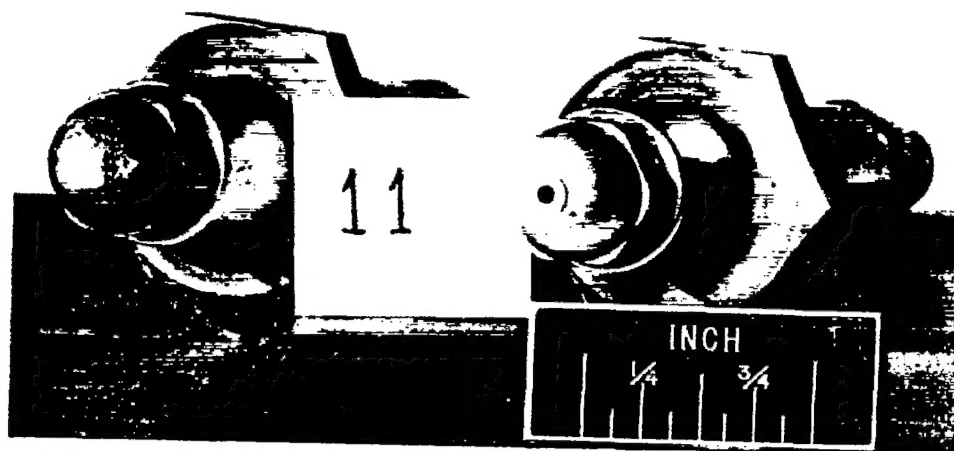
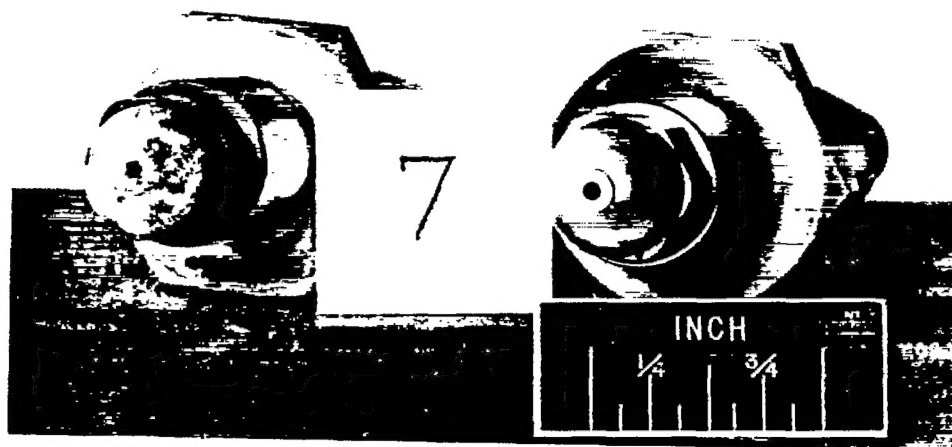
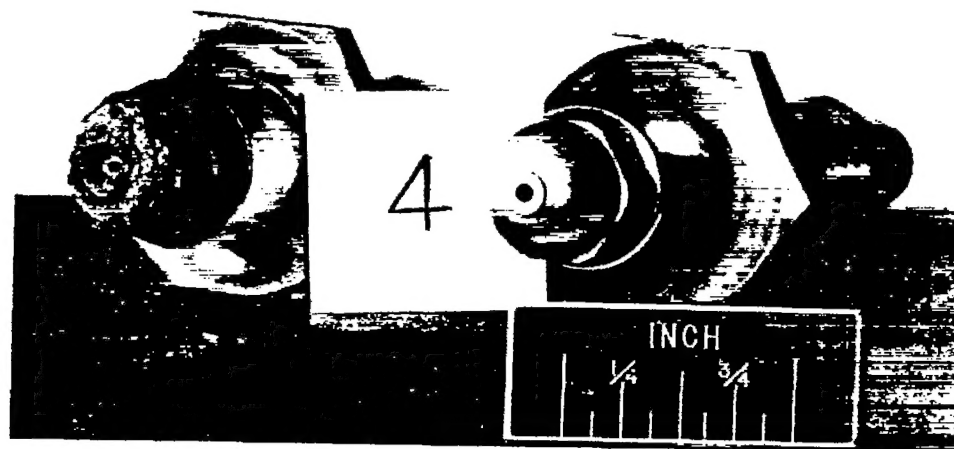


Figure 11. - Fuel nozzles after approximately 1 hour of operation with tributyl borate added to the fuel compared with clean nozzles.